Available online at http://scik.org
Commun. Math. Biol. Neurosci. 2021, 2021:77
https://doi.org/10.28919/cmbn/6586
ISSN: 2052-2541

A DISCRETE-TIME FRACTIONAL-ORDER ROSENZWEIG-MACARTHUR PREDATOR-PREY MODEL INVOLVING PREY REFUGE

HASAN S. PANIGORO*, EMLI RAHMI, NOVIANITA ACHMAD, SRI LESTARI MAHMUD,
R. RESMAWAN, AGUSYARIF REZKA NUHA

Department of Mathematics, Faculty of Mathematics and Natural Sciences,
State University of Gorontalo, Bone Bolango 96119, Indonesia

Abstract. In this article, the dynamical behaviors of a discrete-time fractional-order Rosenzweig-MacArthur model with prey refuge are studied. The piecewise constant arguments scheme is applied to obtain the discrete-time model. All possible fixed points and their existence conditions are investigated as well as the local behavior of nearby solutions in various contingencies. Numerical simulations such as the time series, phase portraits, and bifurcation diagrams are portrayed. Three types of bifurcations are shown numerically namely the forward, the period-doubling, and Neimark-Sacker bifurcations. Some phase portraits are depicted to justify the occurrence of those bifurcations.

Keywords: Rosenzweig-MacArthur; prey refuge; PWCA; bifurcation.
2010 AMS Subject Classification: 92D25, 92D40, 37N25, 39A30, 39A60.

1. INTRODUCTION

The mathematical modeling which studies the interaction among two or more populations with prey and predator relationship has a long history and becomes famous nowadays. Since the classical Lotka-Volterra (1925) [1] and Leslie-Gower models (1948) [2] are proposed, some

*Corresponding author
E-mail address: hspanigoro@ung.ac.id
Received July 30, 2021

predator-prey models are developed by researchers to acquire more realistic models which correspond to the actual circumstances in nature. For example, the predator-prey models involving the Allee effect [3, 4, 5, 6, 7, 8], the fear effect [10, 11, 12, 13, 14], the prey refuge [15, 16, 17], and the combined actions among them [18, 19, 20, 21].

One of the popular predator-prey model is proposed by Rosenzweig and MacArthur (1963) which represents the interaction between a predator and a prey where the prey grows logistically and the predation process following the Holling type-II fuctional response [22]. This model is given by

$$\begin{aligned} \frac{dN}{dt} &= rN\left(1-\frac{N}{K}\right)-\frac{bNP}{1+aN}, \\ \frac{dP}{dt} &= \frac{bcNP}{1+aN}-dP, \end{aligned} \tag{1}$$

where $N(t) \geq 0$ and $P(t) \geq 0$ are prey and predator population densities at time t, respectively. r, k, a, b, c and d are positive constant parameters which have biological interpretation as in the following table.

TABLE 1. The parameters biological interpretation

Parameter	Biological interpretation
r	The intrinsic growth rate of prey
K	The environmental carrying capacity of prey
a	The half saturation constant
b	The attack rate of predator
c	The conversion efficiency of predator on prey
d	The death rate of predator

Naturally, preys try to protect themselves from predators by hiding in a safe areas which knowns as the prey refuge. To include the effect of prey refuge, the model (1) is modified by Kar [23] as follows.

$$\begin{aligned} \frac{dN}{dt} &= rN\left(1-\frac{N}{K}\right)-\frac{b(1-m)NP}{1+a(1-m)N}, \\ \frac{dP}{dt} &= \frac{bc(1-m)NP}{1+a(1-m)N}-dP, \end{aligned} \tag{2}$$

where $m \in (0,1)$ is the refuge protecting constant of prey.

In addition, to establish a more realistic and reliable mathematical model, fractional calculus is regarded as a noteworthy role. The application of fractional calculus in biological modeling swiftly spreading among researchers in consequence of its ability to describe the circumstance more efficiently and accurately [24, 25, 26]. The biological modeling using fractional calculus is considered closer to the actual conditions due to its capability to provides the current states as the impact of all previous biological conditions namely the memory effect [27, 28, 29, 30, 31]. To include the memory effect, the first-order derivatives on the left-hand side of model (2) are replaced by the fractional-order derivative with power-law kernel known as the Caputo operator ${}^{C}\mathscr{D}_{*}^{\alpha}$ which given by the following definition.

Definition 1. [32, 33] Let $f \in C^{n}([0,+\infty),\mathbb{R})$, $\alpha \in (0,1]$ and $\Gamma(\cdot)$ is the Euler's Gamma function. The Caputo fractional derivative of order$-\alpha$ is defined by

$$ {}^{C}\mathscr{D}_{*}^{\alpha} f(t) = \mathscr{I}^{1-\alpha} f'(t)\ t \geq 0, \tag{3} $$

where $\mathscr{I}$ is the Riemann-Liouville fractional integral which given by

$$ \mathscr{I}^{\theta} f(t) = \frac{1}{\Gamma(\theta)} \int_{0}^{t} \frac{f(s)\ ds}{(t-s)^{1-\theta}}. \tag{4} $$

Therefore, we obtain

$$ \begin{aligned} {}^{C}\mathscr{D}_{*}^{\alpha} N(t) &= rN\left(1-\frac{N}{K}\right) - \frac{b(1-m)NP}{1+a(1-m)N}, \\ {}^{C}\mathscr{D}_{*}^{\alpha} P(t) &= \frac{bc(1-m)NP}{1+a(1-m)N} - dP, \end{aligned} \tag{5} $$

Notice that, if the operator of the derivatives are replaced then the dimension of time of eq. (5) at the left-hand side are also changed. There are inconsistency of physical dimensions in eq. (5) where the derivatives at the left-hand side have dimensions of (time)$^{-\alpha}$ while some parameters such as r, b, and d have dimensions of (time)$^{-1}$. This means, by replacing the derivative is not enough to obtain the suitable fractional-order model. To rectify this condition, we rescale the

parameters and obtain the following model.

$$
\begin{aligned}
{}^{C}\mathscr{D}_{*}^{\alpha}N(t) &= r^{-\alpha}N\left(1-\frac{N}{K}\right)-\frac{b^{-\alpha}(1-m)NP}{1+a(1-m)N},\\
{}^{C}\mathscr{D}_{*}^{\alpha}P(t) &= \frac{b^{-\alpha}c(1-m)NP}{1+a(1-m)N}-d^{-\alpha}P,
\end{aligned}
\tag{6}
$$

Now, for simplification, the variables and parameters of model (6) are scaled to obtain the non-dimensional form by assuming $x = N/K$, $y = b^{-\alpha}P/r^{-\alpha}$, and $\tau = r^{-\alpha}t$. Thus, we get

$$
\begin{aligned}
{}^{C}\mathscr{D}_{*}^{\alpha}x(\tau) &= x(1-x)-\frac{(1-m)xy}{1+\omega(1-m)x},\\
{}^{C}\mathscr{D}_{*}^{\alpha}y(\tau) &= \frac{\beta(1-m)xy}{1+\omega(1-m)x}-\delta y,
\end{aligned}
\tag{7}
$$

where $\omega = aK$, $\beta = b^{-\alpha}cK/r^{-\alpha}$, and $\delta = (d/r)^{-\alpha}$. This fractional-order modeling completes the missing step which does not exist in [34]. Nevertheless, the dynamics of model (7) are investigated completely in [34] including the local stability, global stability, the existence of Hopf bifurcation, and supported by their numerical simulations.

Furthermore, although the model with fractional-order derivative is sufficiently enough to investigate the biological process, some researchers prefer to study the predator-prey relationship in a discrete-time model. The discrete-time model is considered suitable to describes most biological processes and gives rich dynamics rather than their continuous ones [35, 36, 37]. Therefore, we are interested to study the dynamics of model (7) in the discrete-time form, where according to the authors' knowledge, the discrete-time model of (7) has never been learned. In this paper, to obtain the discrete-time model, the piecewise constant arguments (PWCA) is employed .

We organize this paper as follows. In Section 2, the discretization process using PWCA is provided. Furthermore, the existence of the fixed points and the dynamics around fixed points are investigated in Section 3. In Section 4, some numerical simulations are performed not only to confirm the analytical findings but also to explore more dynamics of the model such as the existence of forward, period-doubling, and Neimark-Sacker bifurcations. At last, the conclusions of our work are given in Section 5.

2. DISCRETIZATION PROCESS

In this section, we apply the piecewise constant arguments (PWCA) scheme to obtain the discrete form of model (7). By following the similar way in [38, 39, 41, 40], the PWCA of model (7) is given by

$$
\begin{aligned}
{}^{C}\mathscr{D}_{*}^{\alpha}x(\tau) &= x\left(\left[\frac{\tau}{h}\right]h\right)\left(1-x\left(\left[\frac{\tau}{h}\right]h\right)\right)-\frac{(1-m)x\left(\left[\frac{\tau}{h}\right]h\right)y\left(\left[\frac{\tau}{h}\right]h\right)}{1+\omega(1-m)x\left(\left[\frac{\tau}{h}\right]h\right)},\\
{}^{C}\mathscr{D}_{*}^{\alpha}y(\tau) &= \frac{\beta(1-m)x\left(\left[\frac{\tau}{h}\right]h\right)y\left(\left[\frac{\tau}{h}\right]h\right)}{1+\omega(1-m)x\left(\left[\frac{\tau}{h}\right]h\right)}-\delta y\left(\left[\frac{\tau}{h}\right]h\right),
\end{aligned}
\tag{8}
$$

with $x(0)=x_0$ and $y(0)=y_0$ are the initial conditions. For $\tau\in[0,h)$, $\dfrac{\tau}{h}\in[0,1)$, according to eqs. (8), we get

$$
\begin{aligned}
{}^{C}\mathscr{D}_{*}^{\alpha}x(\tau) &= x_0\,(1-x_0)-\frac{(1-m)x_0y_0}{1+\omega(1-m)x_0},\\
{}^{C}\mathscr{D}_{*}^{\alpha}y(\tau) &= \frac{\beta(1-m)x_0y_0}{1+\omega(1-m)x_0}-\delta y_0.
\end{aligned}
\tag{9}
$$

Applying eq. (3) to eqs. (9), we obtain

$$
\begin{aligned}
x_1(\tau) &= x_0+\mathscr{I}^{\alpha}x_0\left[1-x_0-\frac{(1-m)y_0}{1+\omega(1-m)x_0}\right],\\
y_1(\tau) &= y_0+\mathscr{I}^{\alpha}y_0\left[\frac{\beta(1-m)x_0}{1+\omega(1-m)x_0}-\delta\right].
\end{aligned}
\tag{10}
$$

Using eq. (4), eqs. (10) become

$$
\begin{aligned}
x_1(\tau) &= x_0+\frac{\tau^{\alpha}x_0}{\Gamma(1+\alpha)}\left[1-x_0-\frac{(1-m)y_0}{1+\omega(1-m)x_0}\right],\\
y_1(\tau) &= y_0+\frac{\tau^{\alpha}y_0}{\Gamma(1+\alpha)}\left[\frac{\beta(1-m)x_0}{1+\omega(1-m)x_0}-\delta\right].
\end{aligned}
$$

Furthermore, let $\tau\in[h,2h)$, $\dfrac{\tau}{h}\in[1,2)$ and hence eqs. (8) give

$$
\begin{aligned}
{}^{C}\mathscr{D}_{*}^{\alpha}x(\tau) &= x_1\,(1-x_1)-\frac{(1-m)x_1y_1}{1+\omega(1-m)x_1},\\
{}^{C}\mathscr{D}_{*}^{\alpha}y(\tau) &= \frac{\beta(1-m)x_1y_1}{1+\omega(1-m)x_1}-\delta y_1.
\end{aligned}
\tag{11}
$$

Based on eq. (3) the solutions of eqs. (11) are

$$
\begin{aligned}
x_2(\tau) &= x_1 + \mathscr{I}^{\alpha} x_1 \left[1 - x_1 - \frac{(1-m)y_1}{1+\omega(1-m)x_1} \right], \\
y_2(\tau) &= y_1 + \mathscr{I}^{\alpha} y_1 \left[\frac{\beta(1-m)x_1}{1+\omega(1-m)x_1} - \delta \right].
\end{aligned} \tag{12}
$$

Applying eq. (4) to eqs. (12), we obtain

$$
\begin{aligned}
x_2(\tau) &= x_1 + \frac{(\tau-h)^{\alpha} x_1}{\Gamma(1+\alpha)} \left[1 - x_1 - \frac{(1-m)y_1}{1+\omega(1-m)x_1} \right], \\
y_2(\tau) &= y_1 + \frac{(\tau-h)^{\alpha} y_1}{\Gamma(1+\alpha)} \left[\frac{\beta(1-m)x_1}{1+\omega(1-m)x_1} - \delta \right].
\end{aligned}
$$

Now, for $\tau \in [2h, 3h)$, $\dfrac{\tau}{h} \in [2,3)$, eqs. (8) gives

$$
\begin{aligned}
{}^{C}\mathscr{D}_{*}^{\alpha} x(\tau) &= x_2\,(1-x_2) - \frac{(1-m)x_2 y_2}{1+\omega(1-m)x_2}, \\
{}^{C}\mathscr{D}_{*}^{\alpha} y(\tau) &= \frac{\beta(1-m)x_2 y_2}{1+\omega(1-m)x_2} - \delta y_2.
\end{aligned} \tag{13}
$$

By solving eqs. (13) together with eq. (3), we achieve

$$
\begin{aligned}
x_3(\tau) &= x_1 + \mathscr{I}^{\alpha} x_2 \left[1 - x_1 - \frac{(1-m)y_1}{1+\omega(1-m)x_1} \right], \\
y_3(\tau) &= y_1 + \mathscr{I}^{\alpha} y_2 \left[\frac{\beta(1-m)x_1}{1+\omega(1-m)x_1} - \delta \right].
\end{aligned} \tag{14}
$$

Again by utilizing eq. (4), we have solutions for eqs. (14) as follows.

$$
\begin{aligned}
x_3(\tau) &= x_1 + \frac{(\tau-h)^{\alpha} x_2}{\Gamma(1+\alpha)} \left[1 - x_1 - \frac{(1-m)y_1}{1+\omega(1-m)x_1} \right], \\
y_3(\tau) &= y_1 + \frac{(\tau-h)^{\alpha} y_2}{\Gamma(1+\alpha)} \left[\frac{\beta(1-m)x_1}{1+\omega(1-m)x_1} - \delta \right].
\end{aligned}
$$

Repeating the similar process for n-times, we obtain

$$
\begin{aligned}
{}^{C}\mathscr{D}_{*}^{\alpha} x(\tau) =& x_n\,(1-x_n) - \frac{(1-m)x_n y_n}{1+\omega(1-m)x_n}, \\
{}^{C}\mathscr{D}_{*}^{\alpha} y(\tau) =& \frac{\beta(1-m)x_n y_n}{1+\omega(1-m)x_n} - \delta y_n,
\end{aligned} \tag{15}
$$

for $\tau \in [nh,(n+1)h)$, $\dfrac{\tau}{h} \in [n,n+1)$, which according to eq. (3) have solutions

$$\begin{aligned} x_{n+1}(\tau) &= x_n + \mathscr{J}^{\alpha} x_n \left[1 - x_n - \frac{(1-m)y_n}{1+\omega(1-m)x_n}\right], \\ y_{n+1}(\tau) &= y_n + \mathscr{J}^{\alpha} y_n \left[\frac{\beta(1-m)x_n}{1+\omega(1-m)x_n} - \delta\right]. \end{aligned} \tag{16}$$

Obeying eq. (3), we obtain solutions of eqs. (16) as follows.

$$\begin{aligned} x_{n+1}(\tau) &= x_n + \frac{(\tau-nh)^{\alpha} x_n}{\Gamma(1+\alpha)} \left[1 - x_n - \frac{(1-m)y_n}{1+\omega(1-m)x_n}\right], \\ y_{n+1}(\tau) &= y_n + \frac{(\tau-nh)^{\alpha} y_n}{\Gamma(1+\alpha)} \left[\frac{\beta(1-m)x_n}{1+\omega(1-m)x_n} - \delta\right]. \end{aligned} \tag{17}$$

By taking $\tau \to (n+1)h$, eq. (17) yields

$$\begin{aligned} x_{n+1} &= x_n + \frac{h^{\alpha} x_n}{\Gamma(1+\alpha)} \left[1 - x_n - \frac{(1-m)y_n}{1+\omega(1-m)x_n}\right] \equiv F_1(x_n, y_n), \\ y_{n+1} &= y_n + \frac{h^{\alpha} y_n}{\Gamma(1+\alpha)} \left[\frac{\beta(1-m)x_n}{1+\omega(1-m)x_n} - \delta\right] \equiv F_2(x_n, y_n). \end{aligned} \tag{18}$$

If $\alpha \to 1$, we have forward Euler discretization for the first-order derivative model. Furthermore, we investigate the dynamics of model (18) such as the existence of fixed points and their local stability, and some numerical simulations including the local dynamics and the existence of several bifurcations.

3. Fixed Points and Their Local Stability

Now, we study the dynamics of the model (18) including the existence of fixed points and their local stability. The following Lemmas are proposed to espouse our study.

Lemma 1. [40] *Consider a difference equation*

$$x_{n+1} = f(x_n),\ x \in \mathbb{R}^2 \tag{19}$$

A point $x^* \in \mathbb{R}^2$ is called a fixed point of eq. (19) *if satisfies $x^* = f(x^*)$. Suppose that $\lambda_i,\ i = 1,2$ are the eigenvalues of the Jacobian matrix at fixed point x^* of eq.* (19)*. Then the fixed point x^* is*

(i) locally asymptotically stable (sink) if $|\lambda_1| < 1$ and $|\lambda_2| < 1$; or

(ii) unstable (source) if $|\lambda_1| > 1$ and $|\lambda_2| > 1$; or

(iii) unstable (saddle) if $|\lambda_1| < 1$ *and* $|\lambda_2| > 1$*, or* $|\lambda_1| > 1$ *and* $|\lambda_2| < 1$*; or*

(iv) non-hyperbolic $|\lambda_1| = 1$ *and* $|\lambda_2| = 1$.

Lemma 2. [41] *Let* $F(\lambda) = \lambda^2 - Tr\lambda + Det$*. Suppose that* $F(1) > 0$*, and* λ_i*,* $i = 1,2$ *are roots of* $F(\lambda) = 0$*. Then*

(i) $|\lambda_1 < 1|$ *and* $|\lambda_2 < 1|$ *if and only if* $F(-1) > 0$ *and* $Det < 1$.

(ii) $|\lambda_1 > 1|$ *and* $|\lambda_2 > 1|$ *if and only if* $F(-1) > 0$ *and* $Det > 1$.

(iii) $|\lambda_1 < 1|$ *and* $|\lambda_2 > 1|$*, or* $|\lambda_1 > 1|$ *and* $|\lambda_2 < 1|$ *if and only if* $F(-1) < 0$.

(iv) $\lambda_1 = -1$ *and* $\lambda_2 \neq 1$ *if and only if* $F(-1) = 0$ *and* $Tr \neq 0, 2$*, and*

(v) λ_1 *and* λ_2 *are complex and* $|\lambda_1| = |\lambda_2| = 1$ *if and only if* $Tr^2 - 4Det < 0$ *and* $Det = 1$.

Now, we investigate the existence of the fixed point of model (18) by solving the following equations.

$$\begin{aligned} x &= x + \frac{h^\alpha x}{\Gamma(1+\alpha)}\left[1 - x - \frac{(1-m)y}{1+\omega(1-m)x}\right], \\ y &= y + \frac{h^\alpha y}{\Gamma(1+\alpha)}\left[\frac{\beta(1-m)x}{1+\omega(1-m)x} - \delta\right]. \end{aligned} \tag{20}$$

Thus, we obtain three fixed points as follows.

(1) The origin point $E_0 = (0,0)$ which is always exists.

(2) The predator extinction point $E_1 = (1,0)$ which is always exists.

(3) The co-existence point $E^* = \left(x^*, \dfrac{(1-x^*)(1+\omega(1-m)x^*)}{(1-m)}\right)$, where $x^* = \dfrac{\delta}{(\beta - \delta\omega)(1-m)}$, which is exists if $\beta > \dfrac{\delta}{1-m} + \delta\omega$.

Furthermore, the dynamics of these fixed points are presented by the following theorems.

Theorem 3. *Let* $h_0 = \sqrt[\alpha]{\dfrac{2\Gamma(1+\alpha)}{\delta}}$*. The origin point* $E_0 = (0,0)$ *is a source if* $h > h_0$*, a saddle if* $h < h_0$*, and a non-hyperbolic if* $h = h_0$.

Proof. For $E_0 = (0,0)$, we obtain the Jacobian matrix

$$J(E_0) = \begin{bmatrix} 1 + \dfrac{2}{\delta}\left(\dfrac{h}{h_0}\right)^\alpha & 0 \\ 0 & 1 - 2\left(\dfrac{h}{h_0}\right)^\alpha \end{bmatrix},$$

which gives the eigenvalues: $\lambda_1 = 1+\frac{2}{\delta}\left(\frac{h}{h_0}\right)^{\alpha}$ and $\lambda_2 = 1-2\left(\frac{h}{h_0}\right)^{\alpha}$. Since $|\lambda_1|>0$, the fixed point E_0 is always unstable. Furthermore, we use Lemma 1 to identify the type of unstable fixed point E_0. If $h<h_0$ then $|\lambda_2|<1$, and hence E_0 is a saddle point. If $h>h_0$ then $|\lambda_2|>1$, thus E_0 is a source. Finally, if $h=h_0$ then $|\lambda_2|=1$, which means E_0 is non-hyperbolic. □

Theorem 4. *Suppose that* $h_a = \sqrt[\alpha]{2\Gamma(1+\alpha)}$, $h_b = h_a\sqrt[\alpha]{\frac{1+\omega(1-m)}{\delta+(1-m)(\delta\omega-\beta)}}$, *and* $\beta < \frac{\delta}{1-m}+\delta\omega$. *If* $h<\min\{h_a,h_b\}$ *then* E_1 *is a sink, if* $h>\max\{h_a,h_b\}$ *then* E_1 *is a source, if* $h_a<h<h_b$ *or* $h_b<h<h_a$ *then* E_1 *is a saddle, and if* $h=h_a$ *or* $h=h_b$ *then* E_1 *is non-hyperbolic.*

Proof. When $E_1=(1,0)$, the Jacobian matrix is

$$J(E_1) = \begin{bmatrix} 1-2\left(\frac{h}{h_a}\right)^{\alpha} & -\frac{2(1-m)}{1+\omega(1-m)}\left(\frac{h}{h_a}\right)^{\alpha} \\ 0 & 1-2\left(\frac{h}{h_b}\right)^{\alpha} \end{bmatrix},$$

which gives eigenvalues $\lambda_1 = 1-2\left(\frac{h}{h_a}\right)^{\alpha}$ and $\lambda_2 = 1-2\left(\frac{h}{h_b}\right)^{\alpha}$. Since $\beta<\frac{\delta}{1-m}+\delta\omega$, we have $h_b>0$. We can easily proof that if $h<h_a$ then $|\lambda_1|<1$, if $h>h_a$ then $|\lambda_1|>1$, if $h=h_a$ then $|\lambda_1|=1$, if $h<h_b$ then $|\lambda_2|<1$, if $h>h_b$ then $|\lambda_2|>1$, and if $h=h_b$ then $|\lambda_2|=1$. Therefore, by applying Lemma 1, Theorem 4 is well proven. □

Theorem 5. *Suppose that* $2x^*-1>\sqrt{\Delta}$ *and*

$$h_1 = \sqrt[\alpha]{\frac{4\Gamma(1+\alpha)(1-m)\beta x^*}{(1-x^*)\delta+(2x^*-1+\sqrt{\Delta})(1-m)\beta x^*}},$$

$$h_2 = \sqrt[\alpha]{\frac{\Gamma(1+\alpha)\left((1-m)(2x^*-1)\beta x^*+(1-x^*)\delta\right)}{\delta^2(1-x^*)}},$$

$$h_3 = \sqrt[\alpha]{\frac{4\Gamma(1+\alpha)(1-m)\beta x^*}{(1-x^*)\delta+(2x^*-1-\sqrt{\Delta})(1-m)\beta x^*}},$$

$$\Delta = \left(1-2x^*-\frac{(1-x^*)\delta}{(1-m)\beta x^*}\right)^2 - \frac{4(1-x^*)\delta^2}{(1-m)\beta x^*}.$$

Therefore, E^* *is*

(i) sink if $\Delta\geq 0$ *and* $h\in(0,h_1)$, *or* $\Delta<0$ *and* $h\in(0,h_2)$,

(ii) source if $\Delta \geq 0$ *and* $h \in (h_3, +\infty)$*, or* $\Delta < 0$ *and* $h \in (h_2, +\infty)$*,*

(iii) saddle if $\Delta \geq 0$ *and* $h \in (h_1, h_3)$*, and*

(iv) non-hyperbolic if $\Delta \geq 0$ *and* $h = h_1$ *or* $h = h_3$*, or* $\Delta \leq 0$ *and* $h = h_2$*.*

Proof. By computing the Jacobian matrix at E^*, we achieve

$$J(E^*) = \begin{bmatrix} 1 + \dfrac{h^\alpha}{\Gamma(1+\alpha)}\left[1 - 2x^* - \dfrac{\delta(1-x^*)}{\beta(1-m)x^*}\right] & -\dfrac{\delta h^\alpha}{\beta\Gamma(1+\alpha)} \\ \dfrac{\delta(1-x^*)h^\alpha}{\Gamma(1+\alpha)(1-m)x^*} & 1 \end{bmatrix},$$

which gives a quadratic polynomial characteristic $\lambda_2 - Tr(J(E^*))\lambda + Det(J(E^*)) = 0$, where

$$Tr(J(E^*)) = 2 + \frac{h^\alpha}{\Gamma(1+\alpha)}\left[1 - 2x^* - \frac{\delta(1-x^*)}{\beta(1-m)x^*}\right],$$

$$Det(J(E^*)) = 1 + \frac{h^\alpha}{\Gamma(1+\alpha)}\left[1 - 2x^* - \frac{\delta(1-x^*)}{\beta(1-m)x^*}\right] + \frac{h^{2\alpha}(1-x^*)\delta^2}{\Gamma^2(1+\alpha)(1-m)\beta x^*}.$$

Therefore, we obtain two eigenvalues:

$$\lambda_{1,2} = 1 + \frac{h^\alpha}{2\Gamma(1+\alpha)}\left[1 - 2x^* - \frac{\delta(1-x)}{\beta(1-m)x}\right] \pm \frac{h^\alpha\sqrt{\Delta}}{2\Gamma(1+\alpha)}.$$

By utilizing Lemmas 1 and 2, the Theorem 5 is completely proven. □

From the above results, all stability properties of fixed points are influenced by the value of the step-size (h). We confirm that the step-size (h) plays an important role in giving rich dynamical behaviors of model (18). In the next section, we will show numerically that varying step-size (h) also provides more dynamical behaviors namely bifurcations.

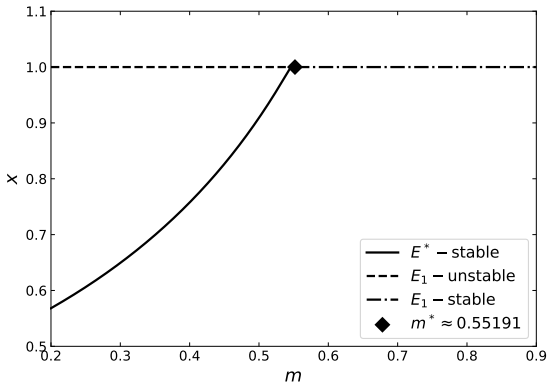

(A) Bifurcation diagram in $(x,m)-$plane

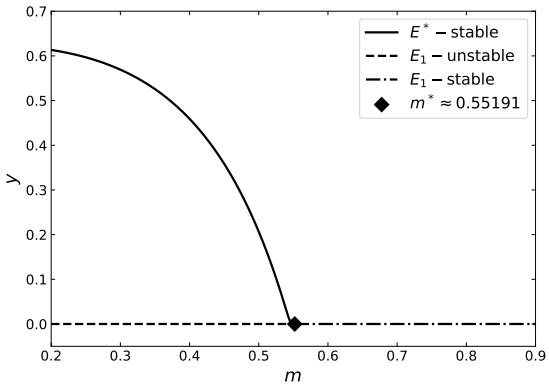

(B) Bifurcation diagram in $(y,m)-$plane

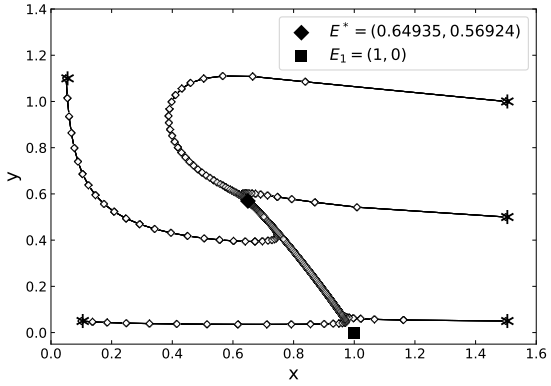

(C) Phase portrait when $m = 0.3$

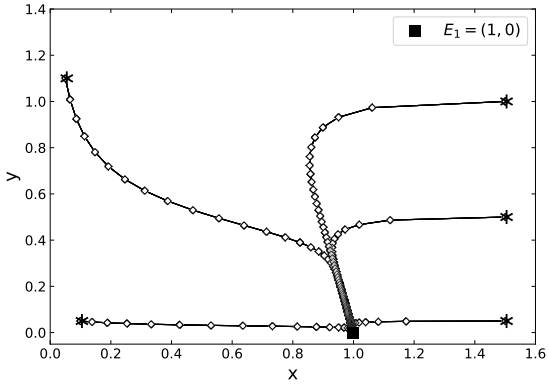

(D) Phase portrait when $m = 0.8$

FIGURE 1. Bifurcation diagram and phase portraits of model (18) with parameter values: $\omega = 0.3$, $\beta = 0.5$, $\delta = 0.2$, $h = 0.4$, and $\alpha = 0.95$.

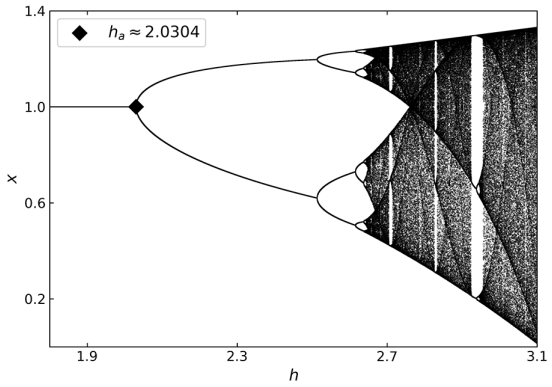

(A) Bifurcation diagram in $1.8 \leq h \leq 3.1$

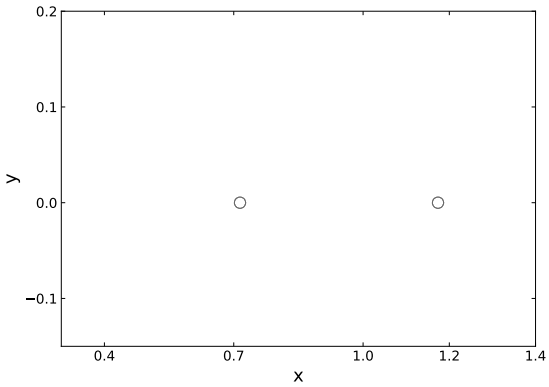

(B) Period-2 solution when $h = 2.3$

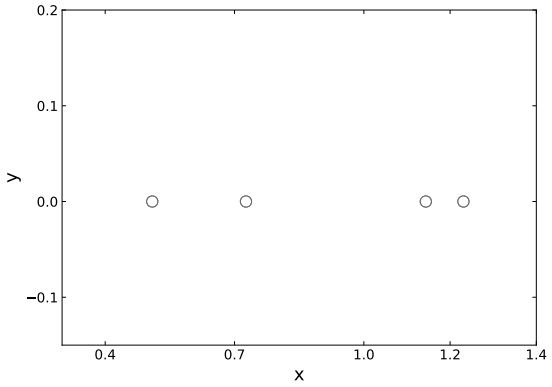

(C) Period-4 solution when $h = 2.61$

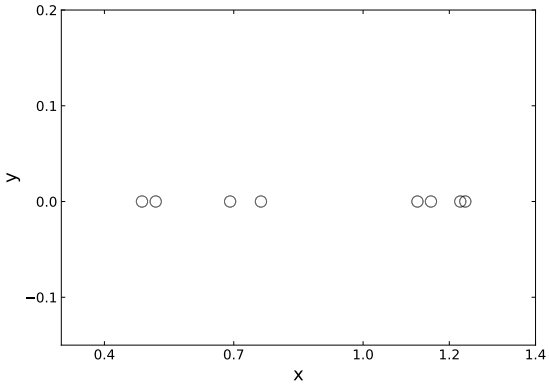

(D) Period-8 solution when $h = 2.63$

FIGURE 2. Bifurcation diagram and periodic solutions around of E_1 with parameter values: $m = 0.8$, $\omega = 0.3$, $\beta = 0.5$, $\delta = 0.2$, and $\alpha = 0.95$.

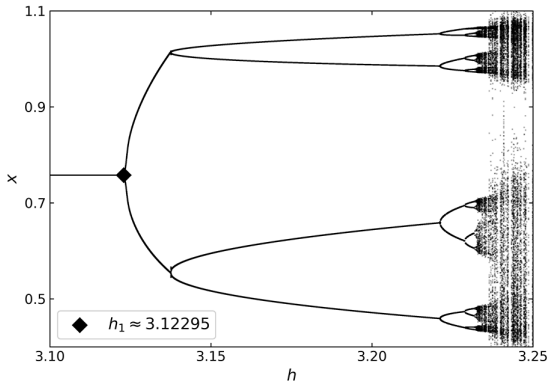

(A) Bifurcation diagram in $3.1 \leq h \leq 3.25$

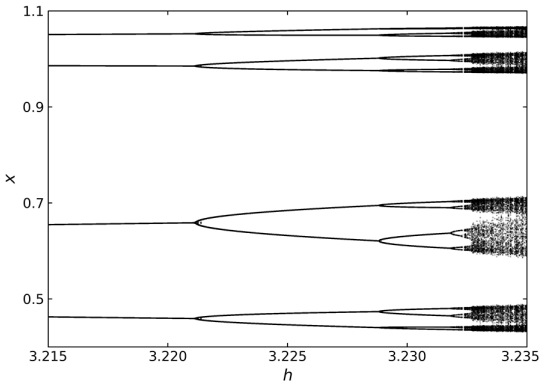

(B) Local amplification to (A)

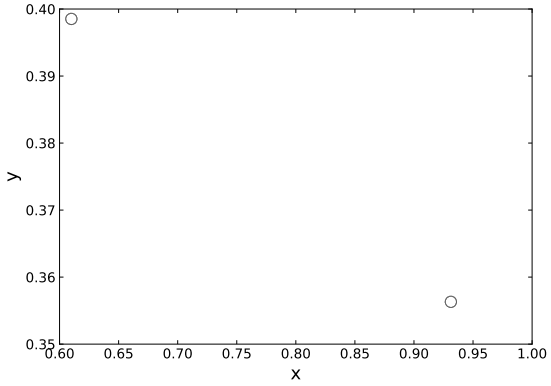

(C) Period-2 solution when $h = 3.13$

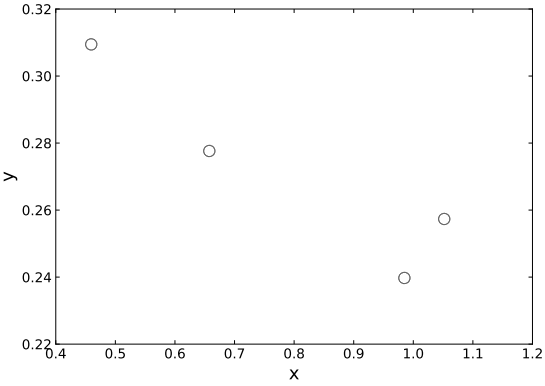

(D) Period-4 solution when $h = 3.22$

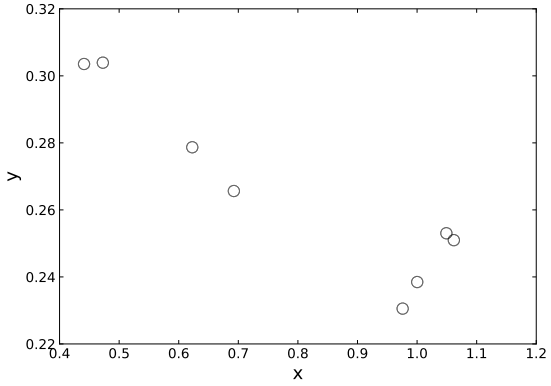

(E) Period-8 solution when $h = 3.228$

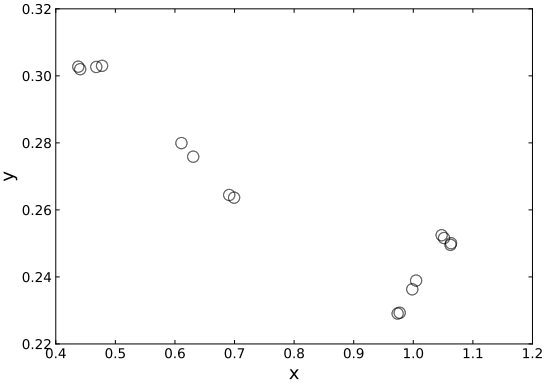

(F) Period-16 solution when $h = 3.23$

FIGURE 3. Bifurcation diagram and periodic solutions around of E^* with parameter values: $m = 0.4$, $\omega = 0.3$, $\beta = 0.5$, $\delta = 0.2$, and $\alpha = 0.95$.

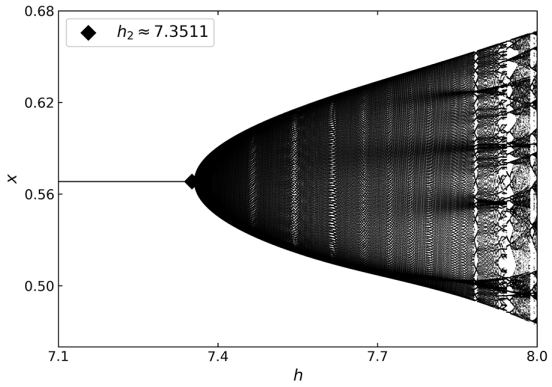

(A) Bifurcation diagram in $7.1 \leq h \leq 8$

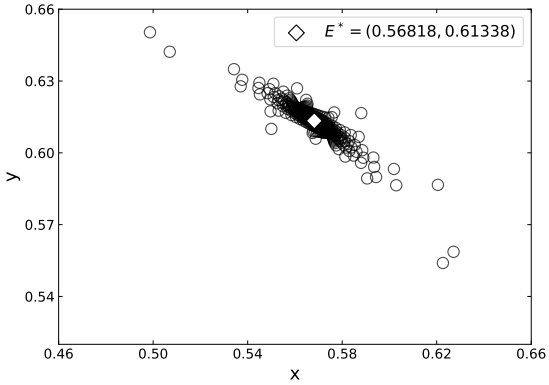

(B) Phase portrait when $h = 7.34$

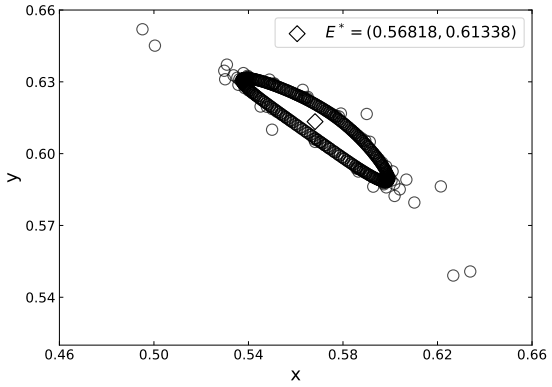

(C) Phase portrait when $h = 7.44$

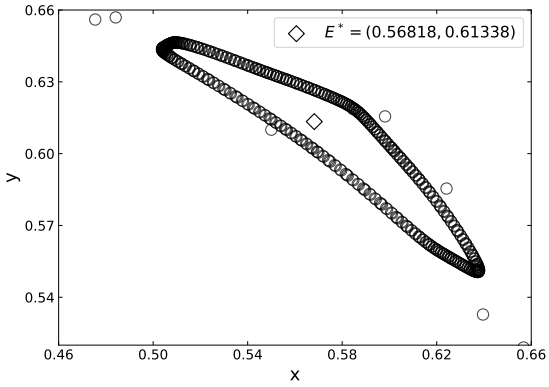

(D) Phase portrait when $h = 7.74$

FIGURE 4. Bifurcation diagram and phase portraits of model (18) with parameter values: $m = 0.2$, $\omega = 0.3$, $\beta = 0.5$, $\delta = 0.2$, and $\alpha = 0.95$.

4. NUMERICAL SIMULATIONS

Some numerical simulations of model (18) are demonstrated. The parameter values are selected hypothetically appropriate with previous analytical results. We first set the parameter values as follows: $\omega = 0.3$, $\beta = 0.5$, $\delta = 0.2$, $h = 0.4$, and $\alpha = 0.95$. By varying the refuge protecting constant of prey (m) in interval $[0.2, 0.9]$, we obtain the bifurcation diagram as in Figures 1a and 1b. When $0.2 \leq m < m^*$, $m^* \approx 0.55191$, we have E_1 and E^* which are unstable and stable respectively. E^* disappeares and E_1 becomes stable via forward bifurcation. We give some phase portraits for each cases in Figures 1c and 1d. When $m = 0.3$, we have an unstable E_1 and a sink E^*. For $m = 0.8$, E^* does not exist and E_1 is a sink.

Furthermore, we investigate the impact of the step-size (h) to the dynamics of each fixed points. First we set the parameter values as used in Figure 1d. Thus, we have a stable fixed point E_1 while E^* does not exist. Now, the step-size is varied in interval $1.8 \leq h \leq 3.1$. We obtain the bifurcation diagram as in Figure 2a. For $1.8 < h < h_a$, $h_a \approx 2.0304$, E_1 is a sink, and loses its stability via period-doubling bifurcation when h passes through h_a. Each branch of stable periodic solutions also bifurcates when h is increased further. To explore the existence of periodic solution, we set the step-size for several values i.e. $h = 2.3, 2.61, 2.63$. We achieve three stable periodic solutions namely period-2,4, and period-8 solutions, see Figures 2b to 2d.

Next, we decrease the value of refuge protecting constant of prey to $m = 0.4$. Therefore, E_1 becomes unstable while E^* is conditionally stable. To investigate the dynamical behaviors around E^* driven by step-size (h), we vary h in interval $[3.1, 3.25]$. We plot the bifurcation diagram in Figure 3a. We show that E^* is a sink when $0 \leq h < h_1$, $h_1 \approx 3.12295$. E^* loses its stability and the period-2 solution occurs when h passes through h_1 which known as period-doubling bifurcation. To more understanding the occurence of periodic solution, we plot the local amplification of bifurcation diagram in Figure 3b. The period-2 solution also bifurcates via period-doubling bifurcation for several times. We plot the periodic solution for $h = 3.13, 3.22, 3.228, 3.23$ to show the existence of period-2,4,8 and period-16 solutions.

Finally, we decrease m to 0.2 and varying h in interval $[7.1, 8]$. When $7.1 \leq h < h_2$, $h_2 = 7.3511$, E^* is a sink. E^* undergoes a Neimark-Sacker bifurcation when h crosses h_2, see Figure 4a. To give a better understanding to the dynamical behavior, we pick some values

of step-size (h) for each cases. When $h = 7.34$, all solutions around E^* convergent to E^* as in Figure 4b. If we increase h to 7.44, E^* loses its stability and nearby solutions convergent to a limit-cycle, see Figure 4c. The diameter of limit-cycle increases when $h = 7.74$ which shown by Figure 4d.

5. CONCLUSIONS

The dynamics of a discrete-time fractional-order Rosenzweig-MacArthur model incorporating a prey refuge which discretized by using piecewise constant arguments have been studied. We achieve three types of fixed points consist of two axial fixed points which always exist, and a conditionally exists interior fixed point. All possible local stability properties are investigated analytically. We show that the integral step-size (h) plays an important role in establishing the dynamical behavior of our model. Finally, we demonstrate numerically the occurrence of several bifurcations. There exists a forward bifurcation driven by the refuge protecting constant of prey (m) which shows the changes in the stability of E_1 and the disappearance of E^* simultaneously when the bifurcations occur. The existence of period-doubling bifurcation also has demonstrated both around E_1 and E^*. Period-2 solution occurs when the step-size (h) is varied. Each periodic solution also experiences period-doubling bifurcations several times. We also show that E^* undergoes a Neimark-Sacker bifurcation driven by time-step (h). From biological meanings, there exist two conditions that may take place in the dynamics of model (18) namely the extinction of predator or the existence of both prey and predator. Especially, the existence of both prey and predator explains in two ways. Both populations will convergent to constant values or change periodically and converge to a periodic solution.

ACKNOWLEDGEMENTS

The authors are grateful to the referees for numerous comments that improved the quality of the paper. Novianita Achmad and Sri Lestari Mahmud are partially funded by FMIPA-UNG via PNBP-State University of Gorontalo according to DIPA-UNG number 305/UN47.B4/HK/2021.

CONFLICT OF INTERESTS

The author(s) declare that there is no conflict of interests.

REFERENCES

[1] A. J. Lotka, Elements of physical biology, Nature 116 (2917) (1925), 461–461.

[2] P. H. Leslie, Some further notes on the use of matrices in population mathematics, Biometrika 35 (3–4) (1948), 213–245.

[3] Y. Cai, C. Zhao, W. Wang, and J. Wang, Dynamics of a Leslie–Gower predator–prey model with additive Allee effect, Appl. Math. Model. 39 (7) (2015), 2092–2106.

[4] E. N. Bodine and A. E. Yust, Predator–prey dynamics with intraspecific competition and an Allee effect in the predator population, Lett. Biomath. 4 (1) (2017), 23–38.

[5] Z. Xiao, X. Xie, and Y. Xue, Stability and bifurcation in a Holling type II predator–prey model with Allee effect and time delay, Adv. Differ. Equ. 2018 (2018), 288.

[6] N. Martínez-Jeraldo and P. Aguirre, Allee effect acting on the prey species in a Leslie–Gower predation model, Nonlinear Anal. Real World Appl. 45 (2019), 895–917.

[7] J. Zhang, L. Zhang, and Y. Bai, Stability and bifurcation analysis on a predator–prey system with the weak Allee effect, Mathematics 7 (5) (2019), 432.

[8] H. S. Panigoro, E. Rahmi, N. Achmad, and S. L. Mahmud, The influence of additive Allee effect and periodic harvesting to the dynamics of Leslie-Gower predator-prey model, Jambura J. Math. 2 (2) (2020), 87–96.

[9] E. Rahmi, I. Darti, A. Suryanto, Trisilowati, and H. S. Panigoro, Stability analysis of a fractional-order Leslie-Gower model with Allee effect in predator, J. Phys. Conf. Ser. 1821 (1) (2021), 012051.

[10] S. Pal, N. Pal, S. Samanta, and J. Chattopadhyay, Fear effect in prey and hunting cooperation among predators in a Leslie-Gower model, Math. Biosci. Eng. 16 (5) (2019) 5146–5179.

[11] D. Mukherjee, Study of fear mechanism in predator-prey system in the presence of competitor for the prey, Ecol. Genet. Genomics 15 (2) (2020), 100052.

[12] S. K. Sasmal and Y. Takeuchi, Dynamics of a predator-prey system with fear and group defense, J. Math. Anal. Appl. 481 (1) (2020), 123471.

[13] Z. Zhu, R. Wu, L. Lai, and X. Yu, The influence of fear effect to the Lotka–Volterra predator–prey system with predator has other food resource, Adv. Differ. Equ. 2020 (2020), 237.

[14] D. Mukherjee, Impact of predator fear on two competing prey species, Jambura J. Biomath. 2 (1) (2021), 1–12.

[15] Y. Li and C. Li, Stability and Hopf bifurcation analysis on a delayed Leslie-Gower predator-prey system incorporating a prey refuge, Appl. Math. Comput. 219 (9) (2013), 4576–4589.

[16] L. K. Beay and M. Saija, A stage-structure Rosenzweig-MacArthur model with effect of prey refuge, Jambura J. Biomath. 1 (1) (2020), 1–7.

[17] M. Moustafa, M. H. Mohd, A. I. Ismail, and F. A. Abdullah, Dynamical analysis of a fractional order eco-epidemiological model with nonlinear incidence rate and prey refuge, J. Appl. Math. Comput. 65(1-2) (2020), 623-650.

[18] H. Zhang, Y. Cai, S. Fu, and W. Wang, Impact of the fear effect in a prey-predator model incorporating a prey refuge, Appl. Math. Comput. 356 (2019), 328–337.

[19] L. Lai, Z. Zhu, and F. Chen, Stability and bifurcation in a predator–prey model with the additive Allee Effect and the fear effect, Mathematics 8 (8) (2020), 1280.

[20] R. Ma, Y. Bai, and F. Wang, Dynamical behavior analysis of a two-dimensional discrete predator-prey model with prey refuge and fear factor, J. Appl. Anal. Comput. 10 (4) (2020), 1683–1697.

[21] D. Barman, J. Roy, H. Alrabaiah, P. Panja, S. P. Mondal, and S. Alam, Impact of predator incited fear and prey refuge in a fractional order prey predator model, Chaos Solitons Fractals 142 (2021), 110420.

[22] M. L. Rosenzweig, R. H. MacArthur, The American Naturalist 97 (895) (1963), 209–223.

[23] T. K. Kar, Stability analysis of a prey–predator model incorporating a prey refuge, Commun. Nonlinear Sci. 10 (6) (2005), 681–691.

[24] M. A. Khan, A. Atangana, Dynamics of ebola disease in the framework of different fractional derivatives, Entropy 21 (3) (2019), 303.

[25] R. Almeida, N. R. O. Bastos, M. T. T. Monteiro, Modeling Some Real Phenomena by Fractional Differential Equations, Math. Methods Appl. Sci. 39 (16) (2016), 4846–4855.

[26] R. Mondal, D. Kesh, D. Mukherjee, Dynamical Analysis of a Fractional Order Rosenzweig-MacArthur Model Incorporating Herbivore Induced Plant Volatile, Chin. J. Phys. 68 (2020), 258–269.

[27] N. Supajaidee, S. Moonchai, Stability analysis of a fractional-order two-species facultative mutualism model with harvesting, Adv. Differ. Equ. 2017 (2017), 372.

[28] H. S. Panigoro, A. Suryanto, W. M. Kusumawinahyu, and I. Darti, A Rosenzweig–MacArthur model with continuous threshold harvesting in predator involving fractional derivatives with power law and Mittag–Leffler kernel, Axioms 9 (4) (2020), 122.

[29] P. Veeresha, D. G. Prakasha, J. Singh, I. Khan, D. Kumar, Analytical approach for fractional extended Fisher–Kolmogorov equation with Mittag-Leffler kernel, Adv. Differ. Equ. 2020 (2020), 174.

[30] H. S. Panigoro, A. Suryanto, W. M. Kusumawinahyu, and I. Darti, Continuous threshold harvesting in a gause-type predator-prey model with fractional-order, AIP Conf. Proc. 2264 (1) (2020), 040001.

[31] H. S. Panigoro, A. Suryanto, W. M. Kusumawinahyu, and I. Darti, Dynamics of an eco-epidemic predator–prey model involving fractional derivatives with power-law and Mittag–Leffler kernel, Symmetry 13 (5), (2021), 785.

[32] I. Petras, Fractional-order nonlinear systems: Modeling, analysis and simulation, Vol. 1, Springer London, Beijing, 2011.

[33] K. Diethelm, The analysis of fractional differential equations: an application-oriented exposition using differential operators of Caputo type, Springer, Braunschweig, 2010.

[34] M. Moustafa, M. H. Mohd, A. I. Ismail, F. A. Abdullah, Dynamical analysis of a fractional-order Rosenzweig–MacArthur model incorporating a prey refuge, Chaos Solitons Fractals 109 (2018), 1–13.

[35] S. M. Salman, On a discretized fractional-order SIR model for Influenza A viruses, Prog. Fract. Differ. Appl. 3 (2) (2017), 163–173.

[36] Y. Lin, Q. Din, M. Rafaqat, A. A. Elsadany, Y. Zeng, Dynamics and Chaos Control for a Discrete-Time Lotka-Volterra Model, IEEE Access 8 (2020), 126760–126775.

[37] H. Cao, H. Wu, X. Wang, Bifurcation analysis of a discrete SIR epidemic model with constant recovery, Adv. Differ. Equ. 2020 (2020), 49.

[38] R. P. Agarwal, A. M. A. El-Sayed, S. M. Salman, Fractional-order Chua's system: discretization, bifurcation and chaos, Adv. Differ. Equ. 2013 (2013), 320.

[39] A. M. El-Sayed, S. M. Salman, On a Discretization Process of Fractional Order Riccati Differential Equation, J. Fract. Calc. Appl. 4 (2) (2013), 251–259.

[40] X. L. Zhuo, F. X. Zhang, Stability for a New Discrete Ratio-Dependent Predator–Prey System, Qual. Theory Dyn. Syst. 17 (1) (2018), 189–202.

[41] M. A. M. Abdelaziz, A. I. Ismail, F. A. Abdullah, M. H. Mohd, Bifurcations and chaos in a discrete SI epidemic model with fractional order, Adv. Differ. Equ. 2018 (2018), 44.

[42] S. N. Elaydi, Discrete chaos: with applications in science and engineering (2nd ed.), Chapman and Hall/CRC, New York, 2007.